

Experimental and theoretical study of $\text{H}+\text{HI}\rightarrow\text{H}_2+\text{I}$ reaction dynamics at 1.3 eV collision energy

Pamela M. Aker, Geoffrey J. Germann, and James J. Valentini

Citation: *The Journal of Chemical Physics* **96**, 2756 (1992); doi: 10.1063/1.462024

View online: <http://dx.doi.org/10.1063/1.462024>

View Table of Contents: <http://scitation.aip.org/content/aip/journal/jcp/96/4?ver=pdfcov>

Published by the AIP Publishing

Articles you may be interested in

Potential energy surfaces and reactive dynamics of $\text{Zn}(3\text{P})$ with H_2

J. Chem. Phys. **105**, 10919 (1996); 10.1063/1.472862

A global H_2O potential energy surface for the reaction $\text{O}(1\text{D})+\text{H}_2\rightarrow\text{OH}+\text{H}$

J. Chem. Phys. **105**, 10472 (1996); 10.1063/1.472977

Quasiclassical trajectory study of the $\text{H}+\text{D}_2\rightarrow\text{HD}+\text{D}$ reaction at a collision energy of 2.2 eV: A comparison with experimental results

J. Chem. Phys. **105**, 6086 (1996); 10.1063/1.472443

Potential energy surface and quasiclassical trajectory studies of the $\text{CN}+\text{H}_2$ reaction

J. Chem. Phys. **105**, 558 (1996); 10.1063/1.471909

Measurement of the statespecific differential cross section for the $\text{H}+\text{D}_2\rightarrow\text{HD}(v'=4, J'=3)+\text{D}$ reaction at a collision energy of 2.2 eV

J. Chem. Phys. **103**, 5157 (1995); 10.1063/1.470604



Experimental and theoretical study of $\text{H} + \text{HI} \rightarrow \text{H}_2 + \text{I}$ reaction dynamics at 1.3 eV collision energy

Pamela M. Aker

Department of Chemistry, University of Wisconsin, Milwaukee, Wisconsin 53211

Geoffrey J. Germann^{a)}

Department of Chemistry, University of California, Irvine, California 92717

James J. Valentini

Department of Chemistry, Columbia University, New York, New York 10027

(Received 27 September 1991; accepted 13 November 1991)

The $\text{H}_2(v', J')$ partial reaction cross sections arising from collisions of 1.3 eV H atoms with HI have been measured using coherent anti-Stokes Raman scattering (CARS) spectroscopy. Quasiclassical trajectory (QCT) calculations on a representative potential energy surface have been used to simulate the dynamics of this reaction. Comparison of the QCT and experimental results shows good agreement in average energy disposal, total cross section, and rotational state distributions. The only significant disagreement is in the detailed vibrational state distribution, for which the calculations give monotonically decreasing population with increasing v' , while the experimental results show a significant population inversion between $v' = 0$ and $v' = 1$. Based on the QCT-experiment comparison we make suggestions for improving the $\text{H} + \text{HI}$ potential energy surface.

I. INTRODUCTION

The high collision energy hydrogen atom abstraction reaction, $\text{H} + \text{HI} \rightarrow \text{H}_2 + \text{I}$, has recently been the focus of experimental studies in this laboratory and others.¹⁻⁶ Interest in the reaction derives in part from the extreme kinematics of the reaction, which is a near perfect example of the light + heavy-light mass combination, and from the extreme energetics of the reaction ($\Delta H = -1.4$ eV), which combined with the high collision energy makes a wide range of product quantum states energetically accessible.⁷ The high collision energy $\text{H} + \text{HI} \rightarrow \text{H}_2 + \text{I}$ reaction has also been the focus of recent quasiclassical trajectory (QCT) studies in our group⁸ and another.^{9,10} The experimental results from different labs are in very good agreement, and overall there is fairly good to very good agreement between the $\text{H}_2(v', J')$ product state distributions derived from the QCT calculations and those reported in state-to-state dynamics experiments.

However, these state-to-state dynamics experiments have one feature that complicates the experiment-theory comparison—the photolysis of HI that is used to generate the reactant H atoms has been affected at 266 nm, a wavelength that yields both $\text{H} + \text{I}(^2P_{3/2})$ and $\text{H} + \text{I}(^2P_{1/2})$, in a ratio of 1.8:1.¹¹⁻¹³ Because of the 0.94 eV energy difference between $\text{I}(^2P_{3/2})$ and $\text{I}(^2P_{1/2})$, the photodissociation thus generates hot H atoms with two substantially different translational energies. This means that the experiments probe the dynamics of the $\text{H} + \text{HI} \rightarrow \text{H}_2 + \text{I}$ reaction at two distinctly different collision energies, 0.7 eV [$\text{H} + \text{I}(^2P_{1/2})$] and 1.6 eV [$\text{H} + \text{I}(^2P_{3/2})$] relative energies. Because of the preponderance of the $\text{H} + \text{I}(^2P_{3/2})$ photolysis channel, the experiments are usually described as being carried out at 1.6 eV (nominal) collision energy. However, there is truly a bimo-

ality of collision energy, and this makes it more difficult to interpret the results of the dynamics experiments at this 1.6 eV (nominal) collision energy, and complicates the comparison with theory. In fact, it is possible that the good agreement observed so far between experimental and theoretical results at the 1.6 eV (nominal) collision energy has been the result of a fortuitous cancellation of errors in the trajectory calculations at the 0.7 eV and 1.6 eV energies needed to describe the experiments.

In an attempt to address and resolve this complication we have both measured and calculated the $\text{H}_2(v', J')$ quantum state distributions from the $\text{H} + \text{HI} \rightarrow \text{H}_2 + \text{I}$ reaction at 1.3 eV collision energy. This particular collision energy has been chosen because it is the closest energy to 1.6 eV (the nominal energy of the previous experiments) that can be achieved under conditions of HI photolysis that give only a single photofragment channel. The 1.3 eV collision energy results from the photolysis of HI at 285 nm, a wavelength at which photodissociation yields only $\text{H} + \text{I}(^2P_{3/2})$ but still in quantities sufficient to carry out state-to-state dynamics experiments.^{11,12}

The experimental data taken at 1.3 eV is quite similar to that measured for reaction at 1.6 eV (nominal) collision energy. Like the 1.6 eV (nominal) results there is generally good agreement with the QCT calculations. However, the 1.3 eV reaction, like the 1.6 eV (nominal) reaction, produces a vibrational population inversion, in contrast to the QCT results, which give a monotonically decreasing population with increasing v' . This discrepancy indicates that the LEPS $\text{H} + \text{HI}$ potential energy surface used in the calculations must be modified, although the modifications that need to be done are not major.

The next section of the paper outlines the experimental and computational methods used in this combined experiment-theory study, and Sec. III describes and compares the results of both the experiments and the QCT calculations. In

^{a)} Present address: IBM Research Division, Almaden Research Center, 650 Harry Road, San Jose, California 95120.

Sec. IV we discuss the implications of the results, particularly in terms of the validity of the QCT description of the state-to-state dynamics and the accuracy of the potential energy surface employed in the calculations, while Sec. V briefly presents our conclusions.

II. METHOD

A. Experiment

Time-resolved coherent anti-Stokes Raman scattering spectroscopy (CARS) was combined with UV photolytic generation of fast H atoms to measure the $\text{H}_2(v', J')$ partial reaction cross sections arising after only one collision of a fast H atom with a 300 K thermal sample of HI. The experimental procedure is essentially identical to that outlined in Ref. 1, except for three details: the UV photolysis wavelength, the reactant gas pressure, and the time delay between the photolysis and probe pulses.

In this experiment, 285 nm UV light, generated by doubling the output of a pulsed dye laser, was used to photolyze HI. At this wavelength the only photofragment channel is $\text{H} + \text{I}(^2P_{3/2})$, giving 1.3 ± 0.1 eV $\text{H} + \text{HI}$ collision energy.^{11,12} The energy spread is due to thermal motion of the 300 K HI sample.¹⁴ The pressure of the reactant HI gas used in this experiment, 3.5 Torr, is lower than that used in Ref. 1, and the time delay, 2.5 ± 0.5 ns, is shorter than that used previously. Our previous experiments were done under near single-collision conditions (total probability of any $\text{H} + \text{HI}$ collision, reactive or nonreactive, ≈ 1); the reduction in sample pressure and probe delay time in the present experiments reduces this probability to ≈ 0.5 .

The vibrational Q-branch CARS spectra of the H_2 product arising from the $\text{H} + \text{HI}$ reaction were analyzed using the procedures outlined in Ref. 1. Both product state distributions and absolute partial cross sections were measured.

B. Quasiclassical trajectory calculations

The dynamics of the 1.3 eV collision energy $\text{H} + \text{HI} \rightarrow \text{H}_2(v', J') + \text{I}$ reaction were modeled by incorporating the LEPS $\text{H} + \text{HI}$ potential of Parr and Kuppermann¹⁵ in the quasiclassical trajectory program of Muckerman,¹⁶ as described in our previous report of QCT calculations on the $\text{H} + \text{HX} \rightarrow \text{H}_2 + \text{X}$ ($\text{X} = \text{Cl}, \text{Br}, \text{I}$) reactions at 1.6 eV (nominal) collision energy.⁸ Details of the LEPS potential surface are given in Ref. 8. Calculations were run using the HI reactant $v = 0, J = 4$ state (the most probable reactant state of the 300 K Boltzmann distribution of the HI sample). Only one reactant rotor state was used in these calculations because our previous studies⁸ showed that reactant rotation has no effect on the dynamics of this reaction at high (> 0.6 eV) collision energy. Nine thousand trajectories were run using a time step of 10 fs, which ensured that energy was conserved to better than one part in 10^4 . The maximum impact parameter used in the calculations was 3.5 Å.

As the trajectory calculations are classical in nature, the rotational state distributions derived from them do not incorporate the different nuclear spin statistics of even J'

($g_{J'} = 1$) and odd J' ($g_{J'} = 3$) H_2 states.^{1,3,4,6} To make the QCT rotational state distributions directly comparable to the experimental rotational state distributions we have therefore multiplied the QCT calculated H_2 even- J' partial reaction cross sections by a factor of $\frac{1}{2}$, and the odd- J' partial reaction cross sections by a factor of $\frac{3}{2}$ to model the restrictions imposed by nature. This scaling introduces the correct spin statistical weighting without altering the total reaction cross section.

III. RESULTS

A. Experiment

Reaction of 1.3 eV H atoms with HI produces H_2 with moderate to large amounts of rotational and vibrational excitation, and the energy disposal is as highly specific as that seen in the 1.6 eV (nominal) collision energy experiment.^{1,6} The rotational and vibrational distributions are quite narrow and exhibit population inversion in both v' and J' . At 1.3 eV collision energy product H_2 vibrational states between $v' = 0$ and 6 can be produced with maximum J' of 21, 19, 17, 14, 11, 8, and 2, respectively, but only a fraction of the allowed states are actually populated.

The measured rovibrational state distributions for the H_2 reaction product at 1.3 eV collision energy are presented in Figs. 1–4. The H_2 reaction product could be observed only in $v' = 0, 1, 2$, and 3. The amount of product in $v' = 4$ must be no more than one third that in $v' = 3$, and less than 2% of the total product yield. Only the odd- J' data are shown in Figs. 1–4. Due to nuclear spin statistics (discussed above) even- J' levels have $\frac{1}{2}$ the population of the odd- J' levels.^{1,3,4,6} The resultant even- J' /odd- J' population alternation makes it harder to compare the 1.3 eV and 1.6 eV (nominal) data as we wish to in the figures, so the even- J' data are not shown. The observed rotational distributions within each vibrational level are narrow, with the population centered around quite highly excited states. The peak of the distributions occurs at $J' = 12, 10, 8$ and 8 in the $v' = 0, 1, 2$, and 3 levels, respectively. The average rotational state populated, $\langle J' \rangle$, is

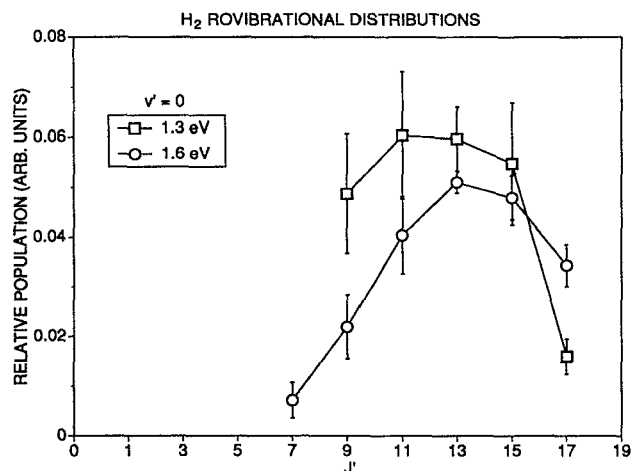


FIG. 1. Comparison of experimentally measured $\text{H} + \text{HI} \rightarrow \text{H}_2(v' = 0, J') + \text{I}$ product rovibrational state distributions at 1.3 eV and 1.6 eV (nominal) collision energies. Only data for odd J' are shown.

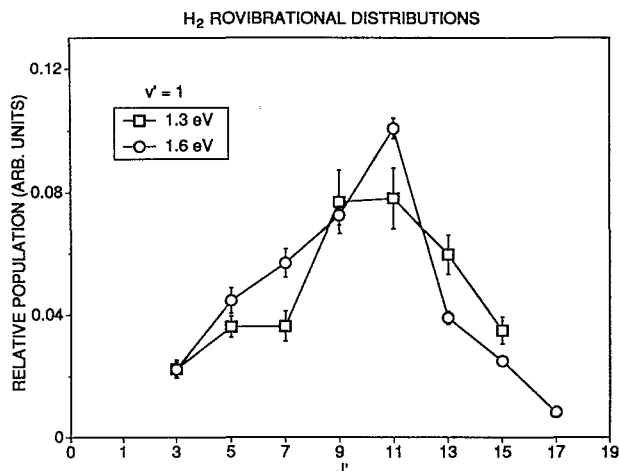


FIG. 2. Comparison of experimentally measured $\text{H} + \text{HI} \rightarrow \text{H}_2 (v' = 1, J') + \text{I}$ product rovibrational state distributions at 1.3 eV and 1.6 eV (nominal) collision energies. Only data for odd J' are shown.

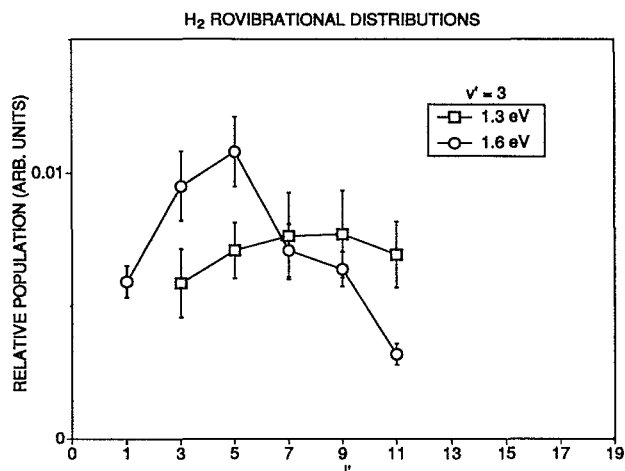


FIG. 4. Comparison of experimentally measured $\text{H} + \text{HI} \rightarrow \text{H}_2 (v' = 3, J') + \text{I}$ product rovibrational state distributions at 1.3 eV and 1.6 eV (nominal) collision energies. Only data for odd J' are shown.

12, 10, 7, and 7, respectively, for the $v' = 0$ to 3 levels. Since the rotational constant for H_2 is large, 60 cm^{-1} , these quantum numbers correspond to a large amount of rotational energy. Table I, which is a summary of the energy disposal observed in the reaction, shows that the fraction of the total available energy partitioned to H_2 product rotation in the 1.3 eV collision energy experiment is 0.25 ± 0.05 .

Also plotted in Figs. 1–4 are the rovibrational state distributions we previously measured for the $\text{H} + \text{HI} \rightarrow \text{H}_2 (v', J') + \text{I}$ reaction at 1.6 eV (nominal) collision energy,¹ and data for the reaction at 1.6 eV are also presented in Table I. The 1.3 eV and 1.6 eV (nominal) data have been normalized such that the sum of the relative populations over v' and J' is the same for both data sets, so the figures compare rovibrational state distributions, corrected for differences in total reactive cross section. A comparison of the experimental data at the two different collision energies shows that the rovibrational state distributions are very

similar, both in terms of the overall fraction of the available energy partitioned to rotation and vibration as well as in the details of the rotational and vibrational state distributions. This comparison must be made cautiously, since the 1.6 eV (nominal) results actually represent contributions from collisions at 0.7 eV and 1.6 eV—the $\text{H} + \text{I}(^2P_{3/2})/\text{H} + \text{I}(^2P_{1/2})$ branching ratio^{11–13} in the 266 nm photolysis of HI implies that 75% of the $\text{H} + \text{HI}$ collisions take place at 1.6 eV and 25% at 0.7 eV. However, we note that the 1.3 eV collision energy is very close to the weighted average of the 0.7 eV and 1.6 eV energies, 1.4 eV, in these earlier experiments.

The f'_v , f'_r , and f'_i values given in Table I differ from those given in Table III of Ref. 7. In that table of Ref. 7 the f'_r and f'_v are interchanged; there f'_r should be 0.25 and f'_v 0.18. Further, the collision energy used to compute E'_{tot} in Ref. 7 was the nominal 1.6 eV collision energy. Here we compute E'_{tot} based on the *average* collision energy, 1.4 eV, that reflects the 75% contribution from collisions at 1.6 eV and 25% contribution from collisions at 0.7 eV. There is only a small quantitative difference between the energy disposal

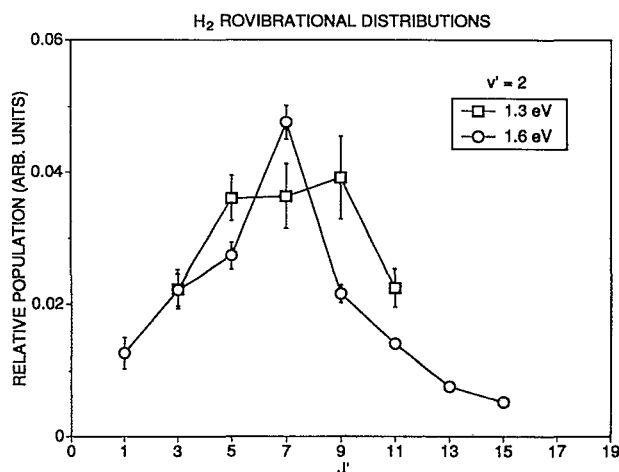


FIG. 3. Comparison of experimentally measured $\text{H} + \text{HI} \rightarrow \text{H}_2 (v' = 2, J') + \text{I}$ product rovibrational state distributions at 1.3 eV and 1.6 eV (nominal) collision energies. Only data for odd J' are shown.

TABLE I. Summary of total cross sections and energy disposal in the $\text{H} + \text{HI} \rightarrow \text{H}_2 + \text{I}$ reaction at high collision energy.

Parameter	1.3 eV experiment	1.3 eV QCT	1.6 eV experiment ^a
E'_{tot} (eV) ^b	2.7	2.7	2.8 ^c
σ (\AA^2)	1.41(35)	1.88(67)	1.10(31)
f'_v	0.19(3)	0.22(2)	0.19(3)
f'_r	0.25(5)	0.25(2)	0.27(5)
f'_i	0.56(6)	0.53(3)	0.53(6)

^a From Ref. 1.

^b The total energy available to the $\text{H}_2 + \text{I}$ products, computed as $D_0(\text{H}_2) - D_0(\text{HI}) + \langle E_{\text{rot}}(\text{HI}) \rangle + E_{\text{rel}} = 1.44 \text{ eV} + E_{\text{rel}}$ for the 300 K thermal HI reactant. See text for details.

^c For this experiment E_{rel} used in calculating E'_{tot} is the average collision energy, based on the 75% contribution from collisions at 1.6 eV and 25% contribution from collisions at 0.7 eV. See text for details.

fractions computed using 1.6 eV or 1.4 eV as the collision energy in our previous experiments, a difference well within the uncertainty in the f'_v values, but using 1.4 eV as the collision energy seems more appropriate given the contribution of both the 0.7 eV and 1.6 eV collisions to the formation of H_2 product.

Reaction of 1.3 eV H atoms with HI produces an H_2 vibrational distribution which, like the H_2 vibrational distribution measured for reaction at 1.6 eV (nominal) collision energy,^{1,6} is inverted and strongly peaked in the $v' = 1$ level. The vibrational distribution, obtained by summing the individual rotational populations in each vibrational level, is $P(v' = 0:1:2:3) = 0.31 \pm 0.08: 0.45 \pm 0.08: 0.20 \pm 0.04: 0.04 \pm 0.01$, and corresponds to an f'_v value of 0.19 ± 0.03 . Within the experimental error, this vibrational distribution is identical with the one we measured¹ for reaction at 1.6 eV (nominal) collision energy $P(v' = 0:1:2:3:4) = 0.27 \pm 0.07: 0.46 \pm 0.07: 0.21 \pm 0.05: 0.05 \pm 0.03: 0.01 \pm 0.01$, from which an f'_v value of 0.27 ± 0.05 is derived.

The similarity of the reaction dynamics at the 1.3 eV and 1.6 eV (nominal) collision energies also extends to the total cross sections. The cross sections are $1.41 \pm 0.35 \text{ \AA}^2$ and $1.10 \pm 0.31 \text{ \AA}^2$, for the 1.3 and 1.6 eV (nominal) energies, respectively. The total cross section quoted here for the 1.6 eV (nominal) collision energy is more precisely specified than the $2 \pm 1 \text{ \AA}^2$ value given by us previously.¹ The increased precision comes from a new and better analysis of the 1.6 eV (nominal) experimental data.

Our QCT results⁸ predict that over the collision energy range 0.7 eV to 1.6 eV the $\text{H} + \text{HI} \rightarrow \text{H}_2 + \text{I}$ reaction cross section should *decrease* with increasing energy. The experimental results presented here are consistent with this prediction, but the cross section change is small compared to the uncertainties, the difference between the collision energies in the two measurements is small, and the 1.6 eV energy is only nominal.

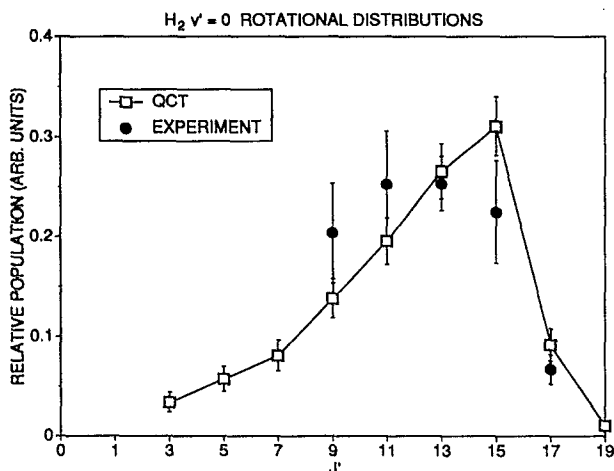


FIG. 5. Comparison of experimentally measured and QCT calculated $\text{H} + \text{HI} \rightarrow \text{H}_2 (v' = 0, J') + \text{I}$ product rotational state distributions at 1.3 eV collision energy. Only data for odd J' are shown.

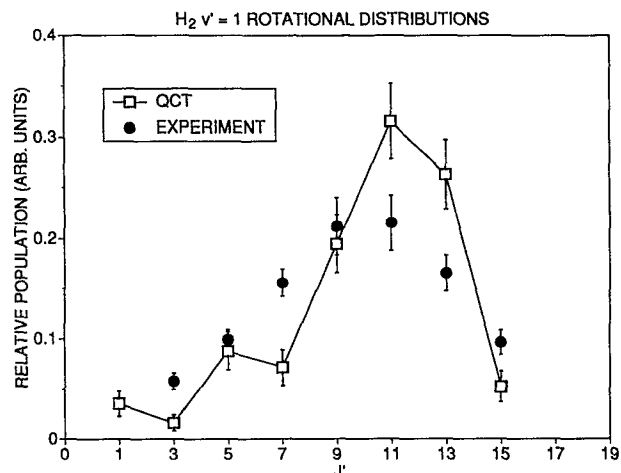


FIG. 6. Comparison of experimentally measured and QCT calculated $\text{H} + \text{HI} \rightarrow \text{H}_2 (v' = 1, J') + \text{I}$ product rotational state distributions at 1.3 eV collision energy. Only data for odd J' are shown.

B. Comparison of theory and experiment at 1.3 eV collision energy

As shown in Table I, the cross section and energy partitioning behavior given by the QCT calculations matches those determined in the 1.3 eV experiment fairly well, at least within the combined QCT (statistical) and experimental uncertainties. The QCT total cross section, $1.88 \pm 0.67 \text{ \AA}^2$ agrees with the $1.41 \pm 0.35 \text{ \AA}^2$ observed, and the f'_v , f'_r , and f'_i values, 0.22 ± 0.02 , 0.25 ± 0.02 , and 0.53 ± 0.03 , respectively, are essentially identical with the 0.19 ± 0.05 , 0.25 ± 0.05 , and 0.56 ± 0.06 values measured in the experiment.

The good agreement between the QCT and experimental results extends beyond these averaged quantities. The detailed rotational state distributions of the QCT calculations

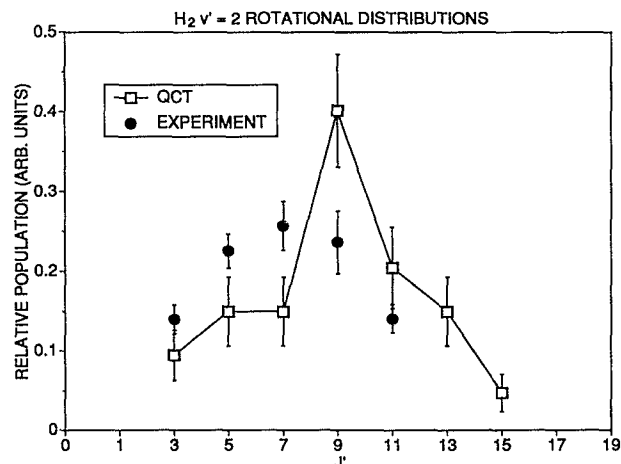


FIG. 7. Comparison of experimentally measured and QCT calculated $\text{H} + \text{HI} \rightarrow \text{H}_2 (v' = 2, J') + \text{I}$ product rotational state distributions at 1.3 eV collision energy. Only data for odd J' are shown.

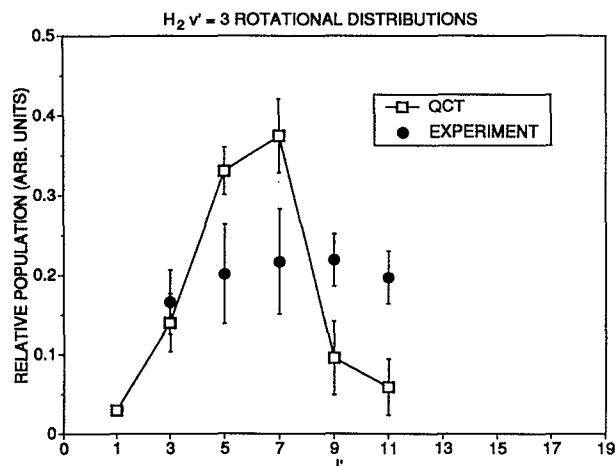


FIG. 8. Comparison of experimentally measured and QCT calculated $\text{H} + \text{HI} \rightarrow \text{H}_2 (v' = 3, J') + \text{I}$ product rotational state distributions at 1.3 eV collision energy. Only data for odd J' are shown.

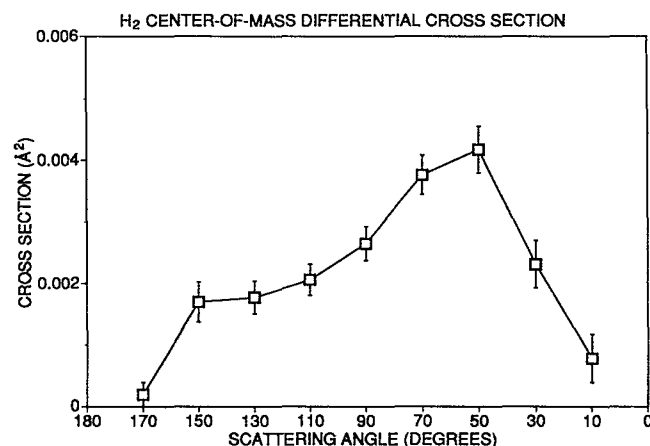


FIG. 10. QCT calculated H_2 product center-of-mass differential cross section for the 1.3 eV collision energy $\text{H} + \text{HI}$ abstraction reaction.

are in quite good agreement with the experiment, as indicated by the theory–experiment comparison in Figs. 5–8. As we did in Figs. 1–4, we present here only the odd- J' data. The experiment–theory comparison is easier to make when the nuclear-spin-statistical even J' /odd J' population alternation is not explicitly shown. The only discrepancy between the QCT and experimental data is a slight shifting of the distribution to higher J' in the calculation as compared to the experiment.

The one significant disagreement between the experimental results and the QCT calculations is in the product vibrational state distributions, which are compared in Fig. 9. The QCT results give a monotonically decreasing vibrational distribution with $P(v' = 0:1:2:3:4:5) = 0.45 \pm 0.12:0.28 \pm 0.09:0.13 \pm 0.06:0.10 \pm 0.05:0.03 \pm 0.02:0.01 \pm 0.01$. In contrast, the experimental $P(v')$ is strongly inverted. The calculations do agree with the experiments in yielding negligible product in $v' > 3$, the highest v' for which H_2 product

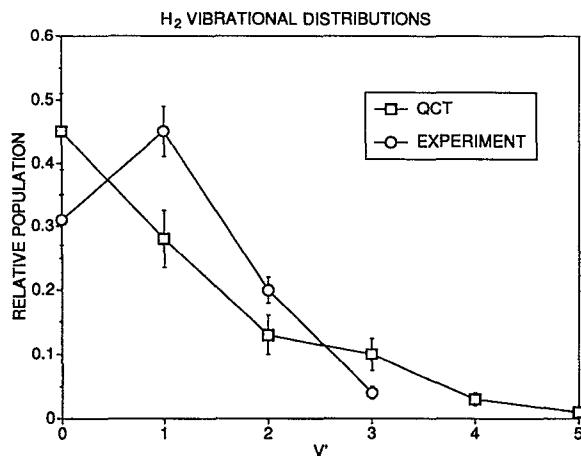


FIG. 9. Comparison of experimentally measured and QCT calculated product vibrational state distributions for the $\text{H} + \text{HI} \rightarrow \text{H}_2 + \text{I}$ reaction at 1.3 eV collision energy.

was observed. This point of agreement should not be overlooked, since $\text{H}_2 v' = 6$ is energetically accessible at 1.3 eV collision energy. Moreover, the average vibrational state of the product, $\langle v' \rangle$ is the same (1.0) for both the QCT and experimental results. However, the detailed $P(v')$ from the QCT calculations is qualitatively different from that actually observed. Exactly the same kind of QCT–experiment discrepancy for $P(v')$ was noted in our previous report of QCT results for 1.6 eV (nominal) collision energy.

Although our CARS experiments are unable to resolve product center-of-mass differential cross sections, we show the results predicted by the QCT calculations for the benefit of those who do perform molecular beam experiments. The center-of-mass differential cross section is calculated using $d\sigma(\theta') = \pi b_{\text{max}}^2 P(\theta') / 2\pi \sin \theta'$, where $P(\theta') = (N_{\text{rxn}}(\theta') / \Delta\theta') / N_{\text{tot}}$. $N_{\text{rxn}}(\theta')$ is the number of abstraction reaction trajectories that scattered into a bin of width $\Delta\theta'$ (here equal to 20°), with θ' the value of the angle at the midpoint of the bin, N_{tot} is the total number of trajectories used in the calculations, and b_{max} is the maximum impact parameter that is included in the calculations. The QCT calculated differential cross section, shown in Fig. 10, indicates that the H_2 product is sideways to forward scattered, with the peak of the distribution occurring at $\theta' \sim 50^\circ$ and the bulk of the population appearing in the forward hemisphere (0° to 90°). As we have discussed previously,⁸ the angular distribution peaks in the forward hemisphere primarily because reaction at large impact parameter is favored in this system, and because the system's collision energy is large.

IV. DISCUSSION

In the 1.3 eV collision energy $\text{H} + \text{HI} \rightarrow \text{H}_2 + \text{I}$ system, the QCT results for the reaction's global parameters—the reaction cross section and energy partitioning—agree quite nicely with the experiment, at least within the combined statistical and experimental uncertainty. Even the details of the H_2 product rotational state distribution are in good agreement. The level and kind of agreement seen in this experiment–theory comparison are the same as those observed in

our previous comparison⁸ of QCT calculations and experiment for this reaction at 1.6 eV (nominal) collision energy. This demonstrates that the previous good agreement was not the result of a fortuitous cancellation of errors in the 0.7 eV and 1.6 eV collision energy calculations needed to make comparison with the experiments.

However, at both 1.3 eV and 1.6 eV (nominal) collision energies there is one important difference between the predictions of the QCT calculations and the experimental observations: the H_2 product vibrational distributions. Experiment reveals an inverted vibrational distribution, with $v' = 1$ populated more highly than $v' = 0$, whereas theory predicts a monotonically decreasing vibrational distribution. However, the average product vibrational quantum number, $\langle v' \rangle$, is 1.0 for both the QCT calculations and the experiments at 1.3 eV. And, in our previous theoretical study of the $\text{H} + \text{HI} \rightarrow \text{H}_2 + \text{I}$ reaction, we showed that the LEPS $\text{H} + \text{HI}$ potential surface did produce a vibrationally inverted H_2 product at the lower collision energy of 0.7 eV.⁸

These results suggest that the LEPS surface is qualitatively correct, but is in its details quantitatively in error. Since no single feature of any potential energy surface controls the vibrational state distribution, particularly when the reaction takes place at a collision energy far in excess of the barrier height as is the case for these studies of the $\text{H} + \text{HI} \rightarrow \text{H}_2 + \text{I}$ reaction, it would be dangerous here to recommend a specific, simple change in the HHI surface to correct the deficiency of the LEPS surface. However, it would seem reasonable as an initial attempt to improve the surface to make the surface less attractive by shifting the barrier a bit toward the exit channel. In fact, González¹⁰ has recently reported getting good agreement between experimental^{1,6} and QCT product vibrational state distributions at 1.6 eV (nominal) energy with a LEPS surface that does just that, shrinking R_{HH} at the saddle point to 1.281 Å from the 1.990 Å of the saddle point in the surface we have used for the QCT calculations here.

V. CONCLUSION

The H_2 product quantum state distributions and partial reaction cross sections for the $\text{H} + \text{HI} \rightarrow \text{H}_2 + \text{I}$ reaction at the single, well-defined collision energy of 1.3 eV have been measured using CARS spectroscopy. Quasiclassical trajectories have been run on a LEPS $\text{H} + \text{HI}$ potential energy surface to simulate the dynamics of the reaction at this high collision energy. The results show the same generally good

theory-experiment agreement for reaction cross sections, product energy disposal, and H_2 rotational state distributions that we observed previously in comparing QCT and experiment at 1.6 eV (nominal) collision energy. This demonstrates that the good agreement between QCT calculations and experiments at this 1.6 eV (nominal) energy, which is a combination of 0.7 eV and 1.6 eV collision energies, is not the result of compensating errors in the calculations at the two energies. At the 1.3 eV energy, as with the 1.6 eV (nominal) energy, there is disagreement of the QCT and experimental product vibrational state distributions. These results suggest that the LEPS potential energy surface is qualitatively correct, but needs some slight modification in detail.

ACKNOWLEDGMENTS

The authors express their appreciation to J. T. Muckerman for providing a copy of his trajectory code, and to A. Kuppermann for supplying the LEPS $\text{H} + \text{HI}$ potential energy surface parameters. This work is supported by the Division of Chemical Sciences, Office of Basic Energy Sciences, Office of Energy Research, U.S. Department of Energy.

- ¹ P. M. Aker, G. J. Germann, and J. J. Valentini, *J. Chem. Phys.* **90**, 4795 (1989).
- ² R. E. Continetti, G. N. Robinson, and Y. T. Lee, poster presented at the 1987 *Conference on the Dynamics of Molecular Collisions*, Wheeling, West Virginia, 1987.
- ³ D. A. V. Kliner, K.-D. Rinnen, and R. N. Zare, *J. Chem. Phys.* **90**, 4625 (1989).
- ⁴ K.-D. Rinnen, D. A. V. Kliner, M. A. Buntine, and R. N. Zare, *Chem. Phys. Lett.* **169**, 365 (1990).
- ⁵ M. A. Buntine, D. P. Baldwin, R. N. Zare, and D. W. Chandler, *J. Chem. Phys.* **94**, 4672 (1991).
- ⁶ D. A. V. Kliner, K.-D. Rinnen, M. A. Buntine, D. E. Adelman, and R. N. Zare, *J. Chem. Phys.* **95**, 1663 (1991).
- ⁷ G. J. Germann and J. J. Valentini, *J. Phys. Chem.* **92**, 3792 (1988).
- ⁸ P. M. Aker and J. J. Valentini, *Isr. J. Chem.* **30**, 157 (1990).
- ⁹ M. González and R. Sayós, *Chem. Phys. Lett.* **164**, 643 (1989).
- ¹⁰ M. González, *J. Chem. Soc. Faraday Discuss.* **92** (1991) (to be published).
- ¹¹ H. Okabe, in *Photochemistry of Small Molecules* (Wiley, New York, 1978).
- ¹² R. D. Clear, S. J. Riley, and K. R. Wilson, *J. Chem. Phys.* **63**, 1340 (1975).
- ¹³ R. Schmiedl, H. Dugan, W. Meier, and K. H. Welge, *Z. Phys. A* **304**, 137 (1982).
- ¹⁴ W. J. van der Zande, R. Zhang, R. N. Zare, K. J. McKendrick, and J. J. Valentini, *J. Phys. Chem.* **95**, 8205 (1991).
- ¹⁵ C. Parr and A. Kuppermann (private communication).
- ¹⁶ J. T. Muckerman (private communication).